EPJ Web of Conferences **314**, 00012 (2024) https://doi.org/10.1051/epjconf/202431400012
QCD@Work 2024

Study of charmonium decays to $K^0_S K\pi$ in the $B \to (K^0_S K\pi)K$ channels

Antimo Palano[1,*]

[1]Istituto Nazionale di Fisica Nucleare, Sezione di Bari, Italy

Abstract. A study of the $B^+ \to K^0_S K^+ K^- \pi^+$ and $B^+ \to K^0_S K^+ K^+ \pi^-$ decays is performed using proton-proton collisions at center-of-mass energies of 7, 8 and 13 TeV at the LHCb experiment. The $K^0_S K^\pm \pi^\mp$ invariant mass spectra from both decay modes reveal a rich content of charmonium resonances, such as η_c, J/ψ, $\eta_c(2S)$ and χ_{c1}. Precise measurements of their parameters and branching fractions are obtained. Dalitz plot analyses of $\eta_c \to K^0_S K^\pm \pi^\mp$ and $\eta_c(2S) \to K^0_S K^\pm \pi^\mp$ decays are performed.

1 Introduction

Light meson spectroscopy in the strange meson sector is still far to be understood, with the only established strange scalar meson being the $K^*_0(1430)$ resonance, whose parameters are yet to be precisely measured [1]. A widely used method of modeling the $K\pi$ S-wave relies on the results from Ref. [2], which consists of a large threshold enhancement described by a scattering length term and a relativistic Breit–Wigner (BW) function describing the $K^*_0(1430)$ resonance. A similar behavior is observed in the $K\pi$ S-wave measured in D^+ decays [3]. Still unresolved is the possible existence of a broad scalar resonance, $\kappa/K^*_0(700)$, claimed by several experiments [1]; its existence would suggest the possible presence of tetraquark states in the light meson system.

2 B^+ signals and measurement of the charmonium resonances parameters

Candidate events are reconstructed and then background suppressed using a multivariate analysis [4]. The resulting $K^0_S K^+ K^- \pi^+$ and $K^0_S K^+ K^+ \pi^-$ mass spectra are shown in Fig. 1, where B^+ signals over small backgrounds can be seen, yielding 74150 and 58460 events, respectively[1]. The corresponding $K^0_S K^\pm \pi^\mp$ mass spectra are shown in Fig. 2. Above the threshold region a D^0 signal is present and prominent η_c, J/ψ, χ_{c1} and $\eta_c(2S)$ resonances are observed.

The measurements of charmonium-resonance parameters are performed with binned fits to the $K^0_S K^\pm \pi^\mp$ invariant-mass spectra separately in the η_c–J/ψ and the χ_{c1}–$\eta_c(2S)$ mass regions. In the fit to the η_c–J/ψ mass region, the J/ψ width is fixed to the known value [1]. All resonances are described by simple non-relativistic BW functions convolved with the appropriate mass resolution functions. The fit results are summarized in Table 1 and show significant improvements with respect to previous measurements. Figure 3 shows the K^+K^-

*e-mail: antimo.palano@ba.infn.it

[1]The inclusion of charge-conjugate processes is implied throughout the paper.

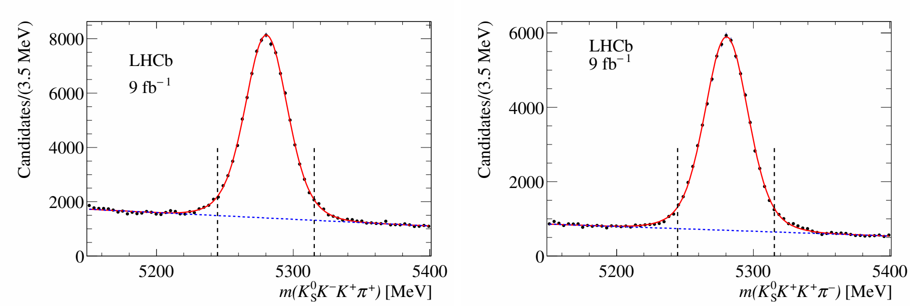

Figure 1. Fitted $K^0_S K^+ K^- \pi^+$ and $K^0_S K^+ K^+ \pi^-$ mass spectra, with indication of signal and background. The vertical lines indicate the B^+ selections.

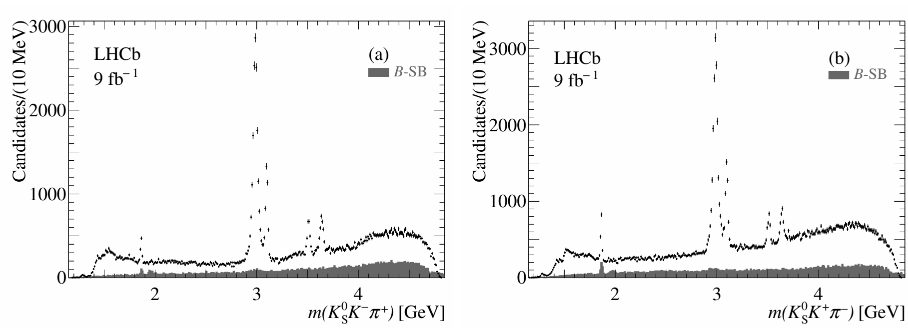

Figure 2. $K^0_S K^\pm \pi^\mp$ mass spectra, from (a) $B^+ \to K^0_S K^+ K^- \pi^+$ and (b) $K^0_S K^+ K^+ \pi^-$. Shaded is the background estimated from B^+ sidebands.

invariant-mass spectrum for $B^+ \to K^0_S K^+ K^- \pi^+$ candidates in the χ_{c0}–χ_{c2} mass region, where a prominent χ_{c0} signal can be seen, together with a weaker signal at the χ_{c2} mass. The $B^+ \to \chi_{c0} K$ decay is expected to be zero in simple factorization models. The χ_{c0} resonance is described by a relativistic spin-0 BW convolved with the experimental resolution and interference is allowed with a non-resonant K^+K^- component. The χ_{c2} parameters are fixed to the known values. The fit returns χ_{c0} parameters consistent with PDG averages with χ_{c0} yield of $N_{\chi_{c0}} = 1920 \pm 90$ and relative phase $\phi = -1.290 \pm 0.073$ rad. The χ_{c2} significance is found to be 4.6σ.

3 Measurements of branching fractions

We use the known PDG η_c and J/ψ branching fractions $B^+ \to (\eta_c/J/\psi)K^+$ as reference and obtain the first branching fractions measurements listed in Table 2. The first uncertainty is statistical, the second systematic, the third is due to the PDG uncertainty on the $B^+ \to \eta_c K^+$ or $B^+ \to J/\psi K^+$ branching fractions.

4 η_c Dalitz plot analysis

Figure 4 shows the $K^0_S K^\pm \pi^\mp$ Dalitz plot in the η_c mass region, separately for $B^+ \to K^0_S K^+ K^- \pi^+$ and $B^+ \to K^0_S K^+ K^+ \pi^-$ data which are dominated by uniform constructive hori-

Table 1. Fitted η_c, J/ψ, $\eta_c(2S)$ and χ_{c1} parameters. The known J/ψ mass is subtracted from the fitted value.

Resonance.	mass (MeV)	width (MeV)	Yield
η_c	$2985.01 \pm 0.17 \pm 0.89$	$29.7 \pm 0.5 \pm 0.2$	34910 ± 283
J/ψ	$-0.54 \pm 0.08 \pm 0.45$	0.0929 (fixed)	6696 ± 106
$\eta_c(2S)$	$3637.90 \pm 0.54 \pm 1.40$	$10.77 \pm 1.62 \pm 1.08$	3680 ± 128
χ_{c1}	$3509.84 \pm 0.69 \pm 0.64$	0.88 (fixed)	2760 ± 86

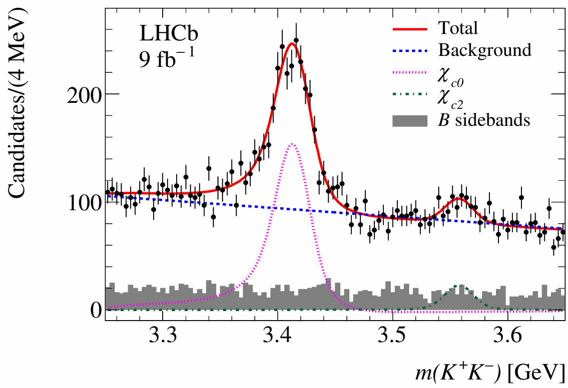

Figure 3. Invariant K^+K^- mass distribution in the χ_{c0}-χ_{c2} mass region for $B^+ \to K^0_S K^+K^-\pi^+$ decays. The results of the fit are overlayed. Superimposed is the K^+K^- invariant-mass spectrum from the B^+ sidebands.

zontal and vertical bands due to the $K^*_0(1430)$ resonance. G-parity relates the final states $\bar{K}^*_0 K$ and $K^*_0\bar{K}$ and, for the I=0 $J^{PC} = 0^{-+}$ η_c resonance, G-parity is even and therefore the $\bar{K}^*_0 K$ and $K^*_0\bar{K}$ bands interfere constructively.

We perform two η_c Dalitz plot analyses. (a) Quasi Model Independent (QMI) measurement of the $K\pi$ S-wave . In this fit, the $K\pi$ invariant-mass spectrum is divided into 37 equally-spaced mass intervals 50MeV wide, and two new fit parameters are added for each interval: the amplitude and phase of the $K\pi$ S-wave. The amplitude is fixed to 1.0 and its phase to $\pi/2$ at an arbitrary point in the mass spectrum, chosen to be interval 16, corresponding to a mass of 1.45 GeV. Other resonant contributions are also added in the fit [4]. Figure 5 shows the fitted $K\pi$ S-wave amplitude and phase obtained from the QMI analysis averaged

Table 2. Measured branching fractions using the η_c (top) or J/ψ (bottom) known branching fractions as reference.

Final state	$\mathcal{B}$ $(\times 10^{-5})$
	η_c as reference
$B^+ \to K^0 K^+ K^- \pi^+$	$32.28 \pm 0.33 \pm 1.97 \pm 7.17$
$B^+ \to K^0 K^+ K^+ \pi^-$	$26.56 \pm 0.31 \pm 0.68 \pm 5.90$
$B^+ \to \chi_{c0} K^0 \pi^+$	$1.38 \pm 0.07 \pm 0.11 \pm 0.32$
$B^+ \to \chi_{c2} K^0 \pi^+$	$0.87 \pm 0.20 \pm 0.08 \pm 0.20$
	J/ψ as reference
$B^+ \to K^0 K^+ K^- \pi^+$	$34.01 \pm 0.74 \pm 0.91 \pm 3.10$
$B^+ \to K^0 K^+ K^+ \pi^-$	$28.01 \pm 0.68 \pm 1.35 \pm 2.55$
$B^+ \to \chi_{c0} K^0 \pi^+$	$1.45 \pm 0.08 \pm 0.11 \pm 0.16$
$B^+ \to \chi_{c2} K^0 \pi^+$	$0.92 \pm 0.21 \pm 0.08 \pm 0.10$

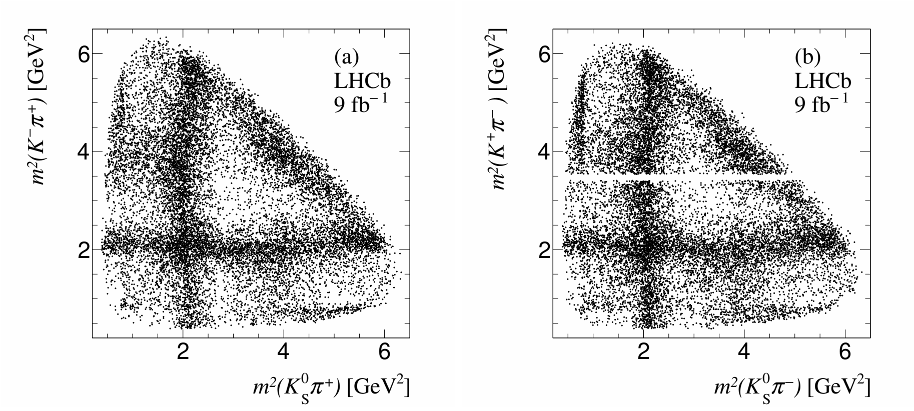

Figure 4. $K^0_S K^\pm \pi^\mp$ Dalitz plot in the η_c mass region, separately for (a) $B^+ \to K^0_S K^+ K^- \pi^+$ and (b) $B^+ \to K^0_S K^+ K^+ \pi^-$ data. A significant $\bar{D}^0 \to K^+\pi^-$ is removed from the $B^+ \to K^0_S K^+ K^+ \pi^-$ data.

over $B^+ \to K^0_S K^+ K^- \pi^+$ and $B^+ \to K^0_S K^+ K^+ \pi^-$ data, which agree well. The data show a dominance of the $K^*_0(1430)$ resonant contribution followed by a sharp drop and a subsequent signal of the $K^*_0(1950)$ resonance. A contribution in the phase motion not continuous with the rest of the distribution is present in the threshold region of Fig. 5(b). This behavior may be attributed to the inability of the algorithm to obtain a correct phase motion in this region of the phase space due to the absence of additional significant resonant contributions.

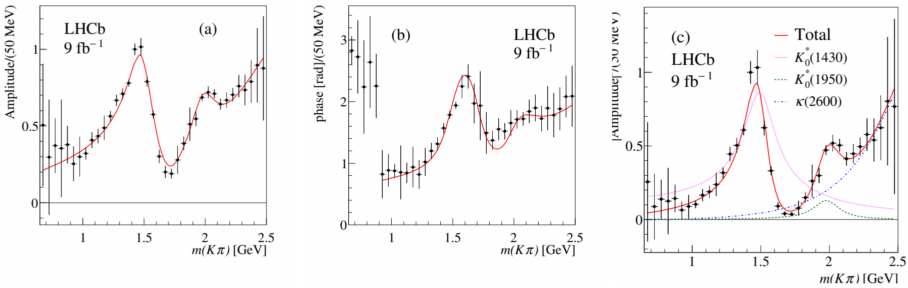

Figure 5. Fit to the (a) amplitude, (b) phase and (c) squared amplitude from the η_c QMI analysis using the results from the isobar-model analysis.

(b) Isobar model. In this fit all the resonances are described by Breit-Wigner functions. The search for the best solution is performed by adding resonances one-by-one, using the $K_0^*(1430)$ resonance as the reference amplitude. It is found that, using only the list of the known resonances, a poor description of the data is obtained. A large improvement (increased likelihood $\Delta(2\log\mathcal{L}) = 1338$) is obtained by adding an additional scalar $K\pi$ resonance with free parameters, labeled in the following as $\kappa(2600)$ and included in the fit using the simple non-relativistic BW function. Resonances having poorly known parameters, namely the $K_0^*(1430)$, $K_0^*(1950)$ and $a_0(1700)$ resonances, are allowed to have free parameters. Table 3 lists the measured resonances parameters where significances are estimated using Wilks' theorem. Table 4 lists the fitted fractional contributions and relative phases obtained by this fitting model and fit projections are shown in Fig. 6. The fit requires the

Table 3. Fitted parameters and significances of the resonances observed in the η_c Dalitz-plot analysis. Significances larger than 10σ are evaluated as $\sqrt{\Delta(2\log\mathcal{L})}$.

Resonance	Mass (MeV)	Γ (MeV)	$\Delta(2log\mathcal{L})$	Significance ($n\sigma$)
$K_0^*(1430)$	$1493 \pm 4 \pm 7$	$215 \pm 7 \pm 4$		
$K_0^*(1950)$	$1980 \pm 14 \pm 19$	$229 \pm 26 \pm 16$	316	17.8
$a_0(1700)$	$1736 \pm 10 \pm 12$	$134 \pm 17 \pm 61$	161	12.7
$\kappa(2600)$	$2662 \pm 59 \pm 201$	$480 \pm 47 \pm 72$	1338	36.6

presence of $a_0(1700)^- \to K_S^0 K^-$, first observed by BaBar ($a_0(1700)^- \to \eta\pi^-$) in the Dalitz plot analysis of $\eta_c \to \eta\pi^+\pi^-$ [5].

We test the consistency between the $K\pi$ $\mathcal{S}-$wave model obtained from the QMI analysis with that obtained from the isobar model analysis. In the isobar model the $K\pi$ $\mathcal{S}-$wave is described in terms of $K_0^*(1430) + K_0^*(1950) + \kappa(2600)$ interfering resonances. We perform a χ^2 fit to the QMI $K\pi$ $\mathcal{S}-$wave amplitude and phase using the model:

$$f(m) = c_1 BW_{K^*(1430)}(m)e^{i\phi_1} + c_2 BW_{K^*(1950)}(m)e^{i\phi_2} + c_3 BW_{\kappa(2600)}(m)e^{i\phi_3}$$

where m indicates the $K\pi$ mass. In this fit, the mass and width of the three resonances are fixed to the results obtained in the isobar model analysis while their coefficients and relative phases are left as free parameters. The fit has a p-value of 63% and is shown in Fig. 5, together with the composition of the fitted resonances. This test shows that the $K\pi$ S-wave obtained using the QMI method can be interpreted as due to the sum of the three interfering K_0^* resonances observed with the isobar model.

Table 4. Results from the Dalitz-plot analysis of the η_c using the isobar model. Inverse-variance-weighted averages from $B^+ \to K_S^0 K^+ K^- \pi^+$ and $B^+ \to K_S^0 K^+ K^+ \pi^-$ data.

Final state	Fraction (%)	Phase [rad]
$K_0^*(1430)\bar{K}$	$33.4 \pm 0.9 \pm 2.0$	0.
$a_0(980)^-\pi^+$	$5.1 \pm 0.5 \pm 0.8$	$-3.38 \pm 0.06 \pm 0.08$
$K_2^*(1420)\bar{K}$	$14.6 \pm 0.7 \pm 0.8$	$3.54 \pm 0.02 \pm 0.07$
$a_2(1310)^-\pi^+$	$1.1 \pm 0.1 \pm 0.2$	$-2.89 \pm 0.08 \pm 0.18$
$K_0^*(1950)\bar{K}$	$3.7 \pm 0.3 \pm 0.2$	$-0.44 \pm 0.04 \pm 0.45$
$a_0(1700)^-\pi^+$	$1.1 \pm 0.2 \pm 0.2$	$1.05 \pm 0.06 \pm 0.15$
$a_0(1450)^-\pi^+$	$2.6 \pm 0.3 \pm 0.5$	$-4.82 \pm 0.06 \pm 0.13$
$a_2(1750)^-\pi^+$	$0.3 \pm 0.1 \pm 0.1$	$2.33 \pm 0.12 \pm 0.11$
$\kappa(2600)\bar{K}$	$61.8 \pm 2.4 \pm 5.4$	$-0.37 \pm 0.03 \pm 0.09$
Sum	$123.7 \pm 2.7 \pm 4.7$	

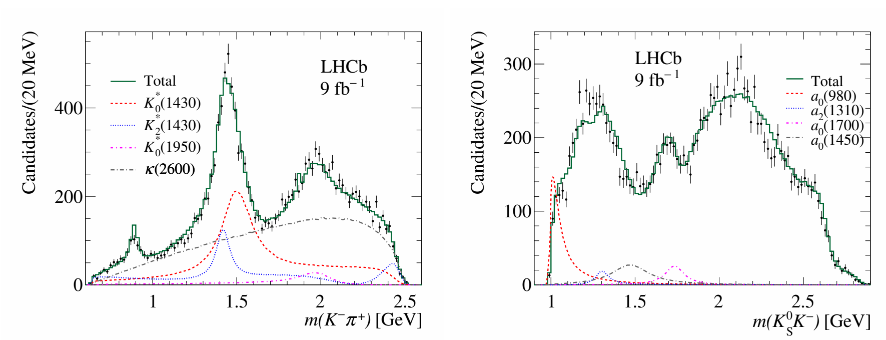

Figure 6. Fit projections on the $K^-\pi^+$, $K_S^0\pi^+$ and $K_S^0K^-$ invariant-mass distributions from the Dalitz-plot analysis of the η_c decay using the isobar model for the $B^+ \to K_S^0 K^+ K^- \pi^+$ data.

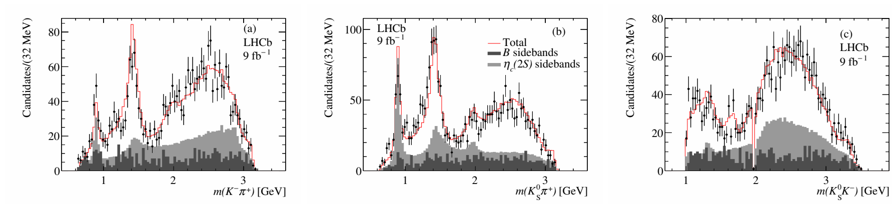

Figure 7. Dalitz-plot projections of the $\eta_c(2S) \to K_S^0 K^\pm \pi^\mp$ decays from the $B^+ \to K_S^0 K^+ K^- \pi^+$ sample. The light gray shaded area is the contribution from the fitted sidebands and the dark shaded gray area is the contribution from the B^+ sidebands.

5 First Dalitz plot analysis of $\eta_c(2S) \to K_S^0 K^\pm \pi^\mp$ in $B^+ \to K_S^0 K^+ K^- \pi^+$

The $\eta_c(2S)$ Dalitz plot is similar to that from the η_c but with larger phase space. To describe the data, we only use the isobar model Dalitz plot analysis with all the resonances parameters fixed to that obtained from the η_c analysis. Fit projections are shown in Fig. 7 and results are listed in Table 5. We note large interference effects and similar features as for the η_c analysis, including a small enhancement at the position of the $a_0(1700)$ resonance.

Table 5. Results from the Dalitz-plot analysis of $\eta_c(2S) \to K^0_S K^\pm \pi^\mp$ in the $B^+ \to K^0_S K^+ K^- \pi^+$ final state using the isobar model.

Final state	Fraction [%]	Phase [rad]
$K_0^*(1430)K$	$25.5 \pm 3.3 \pm 4.1$	0.
$K_2^*(1430)K$	$24.5 \pm 3.3 \pm 4.4$	$3.10 \pm 0.11 \pm 0.08$
$K_0^*(1950)K$	$3.7 \pm 1.3 \pm 1.1$	$-0.82 \pm 0.17 \pm 0.24$
$a_0(1700)^-\pi^+$	$1.7 \pm 1.1 \pm 0.5$	$1.22 \pm 0.32 \pm 0.90$
$a_0(1450)^-\pi^+$	$7.8 \pm 1.9 \pm 1.0$	$1.86 \pm 0.14 \pm 0.56$
$a_2(1750)^-\pi^+$	$4.9 \pm 1.4 \pm 1.1$	$-1.75 \pm 0.15 \pm 0.39$
$\kappa(2600)K$	$124.2 \pm 9.0 \pm 7.7$	$-0.91 \pm 0.10 \pm 0.08$
Sum	$192.3 \pm 10.9 \pm 10.0$	

Table 6. Inverse-variance-weighted averages of the fractional contributions for χ_{c1} decays to $K^*\bar{K}$ resonances from the $B^+ \to K^0_S K^+ K^- \pi^+$ and $B^+ \to K^0_S K^+ K^+ \pi^-$ final states. The reported uncertainties are statistical, systematic and from the uncertainty on the χ_{c1} branching fraction.

Decay mode	Fraction	Branching fraction ($\times 10^{-3}$)
$\mathcal{B}(\chi_{c1} \to K^*(892)^0 \bar{K}^0)$	$0.099 \pm 0.012 \pm 0.004$	$1.04 \pm 0.13 \pm 0.04 \pm 0.09$
$\mathcal{B}(\chi_{c1} \to K_2^*(1430)^0 \bar{K}^0)$	$0.111 \pm 0.015 \pm 0.005$	$1.17 \pm 0.16 \pm 0.05 \pm 0.10$
$\mathcal{B}(\chi_{c1} \to K^*(892)^+ K^-)$	$0.112 \pm 0.016 \pm 0.013$	$1.18 \pm 0.17 \pm 0.14 \pm 0.10$
$\mathcal{B}(\chi_{c1} \to K_2^*(1430)^+ K^-)$	$0.143 \pm 0.018 \pm 0.006$	$1.61 \pm 0.19 \pm 0.19 \pm 0.14$

6 Study of the χ_{c1} decay to $K^0_S K^\pm \pi^\mp$

The χ_{c1} Dalitz plot for $B^+ \to K^0_S K^+ K^- \pi^+$ data, is dominated by the presence of $K^*(892)$ and $K_2^*(1430)$ resonances. A fit to the $K\pi$ and $K^0_S\pi$ invariant-mass distributions is performed using an empirical background shape in addition to two relativistic BW functions describing the $K^*(892)$ and $K_2^*(1430)$ resonances with parameters fixed to their known values. The fractional $K^*(892)$ and $K_2^*(1430)$ contributions are converted into $\chi_{c1} \to K^*\bar{K}$ branching fractions, listed in Table 6, by multiplying the fractional contributions by the known χ_{c1} branching fraction, $\mathcal{B}(\chi_{c1} \to \bar{K}^0 K^+ \pi^-) = (7.0 \pm 0.6) \times 10^{-3}$ [1] and correcting for unseen K^* decay modes. We obtain branching fractions determinations with improved precision with respect to previous measurements.

References

[1] S. Navas *et al.* [Particle Data Group], "Review of particle physics,", Phys. Rev. D **110** (2024) no.3, 030001. https://doi:10.1103/PhysRevD.110.030001

[2] D. Aston *et al.* "A Study of $K^-\pi^+$ Scattering in the Reaction $K^-p \to K^-\pi^+n$ at 11-GeV/c," Nucl. Phys. B **296** (1988), 493-526 https://doi:10.1016/0550-3213(88)90028-4

[3] E. M. Aitala *et al.* [E791], "Model independent measurement of S-wave $K^-\pi^+$ systems using $D^+ \to K^-\pi^+\pi^+$ decays from Fermilab E791," Phys. Rev. D **73** (2006), 032004 [erratum: Phys. Rev. D **74** (2006), 059901] https://doi:10.1103/PhysRevD.73.032004

[4] R. Aaij *et al.* [LHCb], "Study of charmonium decays to $K^0_S K\pi$ in the $B \to (K^0_S K\pi)K$ channels," Phys. Rev. D **108** (2023) no.3, 032010 https://doi:10.1103/PhysRevD.108.032010

[5] J. P. Lees *et al.* [BaBar], "Light meson spectroscopy from Dalitz plot analyses of η_c decays to $\eta' K^+ K^-$, $\eta'\pi^+\pi^-$, and $\eta\pi^+\pi^-$ produced in two-photon interactions," Phys. Rev. D **104** (2021) no.7, 072002 https://doi:10.1103/PhysRevD.104.072002